Title
Arctic mercury depletion and its quantitative link with halogens

Journal
Journal of Atmospheric Chemistry, 65(2-3)

ISSN
0167-7764

Authors
Mao, Huiting
Talbot, Robert W
Sive, Barkley C
et al.

Publication Date
2010-04-01

DOI
10.1007/s10874-011-9186-1

J Atmos Chem (2010) 65:145–170
DOI 10.1007/s10874-011-9186-1

Arctic mercury depletion and its quantitative link with halogens

Huiting Mao · Robert W. Talbot · Barkley C. Sive · Su Youn Kim · Donald R. Blake · Andrew J. Weinheimer

Received: 30 June 2010 / Accepted: 17 March 2011 /
Published online: 7 April 2011

Abstract Gas phase elemental mercury (Hg°) was measured aboard the NASA DC-8 research aircraft during the Arctic Research of the Composition of the Troposphere from Aircraft and Satellites (ARCTAS) campaign conducted in spring 2008 primarily over the North American Arctic. We examined the vertical distributions of Hg° and ozone (O_3) together with tetrachloroethylene (C_2Cl_4), ethyne (C_2H_2), and alkanes when Hg°- and O_3-depleted air masses were sampled near the surface (<1 km). This study suggests that Hg° and O_3 depletions commonly occur over linear distances of ~20–200 km. Horizontally there was a sharp decreasing gradient of ~100 ppqv in Hg° over <10 km in going from the bay near Ellesmere Island to the frozen open ocean. There was a distinct land-ocean difference in the vertical thickness of the Hg°-depleted layer – being variable but around a few 100 meters over the ocean whereas occurring only very near the surface over land. Data

Electronic supplementary material The online version of this article (doi:10.1007/s10874-011-9186-1) contains supplementary material, which is available to authorized users.

H. Mao (✉)
Department of Chemistry, State University of New York College of Environmental Science and Forestry, One Forestry Drive, Syracuse, New York 13210, USA
e-mail: hmao@esf.edu

R. W. Talbot
Department of Earth and Atmospheric Sciences, University of Houston, Houston, TX 77204–5007, USA

B. C. Sive
Institute for the Study of Earth, Oceans, and Space, Climate Change Research Center, University of New Hampshire, Morse Hall, 8 College Road, Durham, NH 03824, USA

S. Youn Kim
Department of Soil, Water, and Climate, University of Minnesota, St. Paul, MN 55108–6028, USA

D. R. Blake
Department of Chemistry, University of California – Irvine, Irvine, CA 92697–2025, USA

A. J. Weinheimer
National Center for Atmospheric Research, Earth and Sun Systems Laboratory, P.O. Box 3000, Boulder, CO 80307–3000, USA

support that atmospheric mercury depletion events are driven by Hg° reactions with halogen atoms. Derived from data collected aboard the DC-8, we present mathematical expressions giving the rates of Hg° and O_3 depletions as a function of the radical concentrations. These relationships can be a useful metric to evaluate models that attempt to reproduce springtime Arctic Hg° and/or O_3 depletion events, and they can also be employed to obtain order-of-magnitude estimates of radical concentrations and the ratio [Br]/[Cl].

Keywords ARCTAS · Arctic spring · Mercury depletion event · Ozone depletion event · Halogens

1 Introduction

The sources and sinks of atmospheric mercury (Hg), a serious environmental toxin, are poorly characterized and quantified. More than a decade has been devoted to understanding the loss mechanisms of gaseous elemental mercury (Hg°) in the Arctic spring since Schroeder et al. (1998) first reported a rapid surface level decrease following polar sunrise. Theoretical and laboratory studies speculate that Hg° is oxidized by halogens, primarily atomic bromine (Br) and bromine monoxide (BrO) (Ariya et al. 2002; Ariya et al. 2004; Calvert and Lindberg 2003; Goodsite et al. 2004) derived from sea-salt aerosols over open sea water (von Glasow 2008). Supportive evidence from field measurements show concomitant decreases in Hg° and peaks in reactive gaseous mercury (RGM), particulate mercury (Hg^P) and BrO (Lu et al. 2001; Lindberg et al. 2001; Brooks et al. 2006). More direct, intrinsic evidence is needed to demonstrate the important role of halogen radicals in Hg cycling.

Previous studies suggested that chlorine (Cl) and Br chemistries are also responsible for loss of volatile organic compounds (VOCs) in Arctic spring. It was found that during Arctic O_3 depletion events (ODEs) all alkanes and ethyne displayed substantial decreases in their mixing ratios, of which alkanes and toluene were consistent with the occurrence of Cl reactions (Jobson et al. 1994; Ariya et al. 1999; Bottenheim et al. 1990, 2002; Eneroth et al. 2007). A significant positive correlation was also found between acetaldehyde and O_3, which is speculated to result from oxidation by Br atoms, and a negative correlation between acetone and O_3 due possibly to enhanced production of acetone from gas-phase oxidation of propane by Cl atoms (Boudries et al. 2002). Occurrences of Hg° and O_3 depletion events have been observed in synchronization annually throughout maritime circumpolar sites (Schroeder et al. 1998; Lindberg et al. 2001; Skov et al. 2004; Berg et al. 2003; Ebinghaus et al. 2002). Given the correlation between O_3 and VOCs during ODEs, it would be interesting to examine the relationship, if any exists, between Hg° and VOCs during Arctic mercury depletion events (AMDEs).

Tropospheric measurements of the vertical distribution of Hg° are sparse, and the majority have been obtained from research aircraft primarily below 8 km (Ebinghaus and Slemr 2000; Banic et al. 2003; Friedli et al. 2004; Radke et al. 2007; Swartzendruber et al. 2008). The vertical profiles from 0.1 km to 7 km altitude reported by Banic et al. (2003) showed depletion of elemental mercury near the surface with mixing of depleted air to altitudes of 1 km. The balloon measurements conducted by Tackett et al. (2007) suggested that Hg° depletion occurred with the lowest 100 m layer. More knowledge of the vertical structure of AMDEs is needed to understand the phenomenon thoroughly.

During the Arctic Research of the Composition of the Troposphere from Aircraft and Satellites (ARCTAS) campaign, the latest airborne campaign of the Tropospheric Chemistry

Program at the National Aeronautics and Space Administration, it was the first time that Hg° was measured together with numerous other trace gases from an aircraft in the springtime Arctic. Our goal was to conduct an integrated examination of the relationships between Hg°, O_3, and VOCs during Hg° and O_3 depletion events using continuous measurements from an airborne platform to obtain an analysis. Thus, we first present the airborne observations that show depletion of Hg°, O_3, and selected VOCs over the frozen open ocean and obtain its vertical and horizontal extent. This is followed by an analysis of the observational data from all depletion events to derive mathematical expressions of the observed Hg° and O_3 depletion rates.

2 Measurements and data

ARCTAS was conducted in spring/summer 2008 primarily over the North American Arctic with a flight package that included in situ Hg° measurements. All ARCTAS flight tracks are shown in Figure S1. We incorporated a modified Tekran 2537A cold vapor atomic fluorescence spectrometer with pressure control into the University of New Hampshire (UNH) DC-8 measurement package (Talbot et al. 2008). Mixing ratios of Hg° were measured with 140 s time response. Mercury-free zero air was generated onboard the DC-8 using cabin air and our own Hg-stripping cartridge train assembly. Standard addition calibrations were conducted on ambient air using an internal Hg° permeation source. On non-flight days these were conducted on the ground and then on every science flight at altitudes ranging from 1 to 12 km. Instrument calibration was cross-checked using injections from the headspace of a thermoelectrically cooled Hg° reservoir (Tekran model 2505). This was done during instrument integration prior to field deployment, and then again back at UNH after ARCTAS was completed. The calibration was reproducible to within ±3% over this 4 month time period. Correspondingly, the response factor of the instrument (peak area counts pg^{-1} Hg°) was constant to ±1% for the entire data set. The estimated precision of the Hg° measurements was 10–15%, with a limit of detection of ~10 ppqv. For presentation in this paper we assigned Hg° mixing ratios below the limit of detection a value of zero to emphasize the depletion. However, in linear correlation analysis for this work these zero values were ignored and only measured values of Hg° were utilized.

The inlet arrangement is crucial for reliable measurements of atmospheric mercury. We utilized our existing high flow inlet (1,500 standard liters per minute) for nitric acid (Talbot et al. 2008). It is designed specially for the DC-8 with a diffuser that boosts the pressure inside the inlet by up to 100 mbar over ambient. For the Hg° measurements the high flow air stream was sub-sampled through a heated (40°C) PFA Teflon line just a few centimeters after the flow entered the main 10 cm diameter manifold (Talbot et al. 2007).

Ozone was measured at 1 Hz using the chemiluminescence technique with a detection limit of better than 0.1 ppbv, as described in Ridley et al. (1992). Measurements of VOCs were conducted by the University of California at Irvine. During the sampling the canisters were pressurized to 40 psi using a metal double bellows pump. The filling time was approximately 1 minute. Canisters were filled at 1–3 min intervals during ascents and descents, and every 2–8 min during horizontal flight legs. A maximum of 168 canisters were filled for each flight. Filled canisters were shipped within 7 days of sample collection back to the UC-Irvine laboratory where they were analyzed for more than 75 gases including nonmethane hydrocarbons, halocarbons, alkyl nitrates and sulfur compounds. A detailed description of the analytical system is described in Colman et al. (2001).

Ten day kinematic backward trajectories were provided by Florida State University (Fuelberg et al. 1996 2000; Martin et al. 2002). The 1 h interval trajectories at every minute of the flight location were calculated by FSU-WRF winds at 45 km resolution. In this study we used the first five days of trajectories to be cautious.

3 Variation in Hg°, O_3, and VOCs during AMDEs and ODEs

All of the measurement data from the entire spring deployment is presented in Fig. 1 except samples south of 50°N, which were collected on Fight #1 on 1 April 2008 and Flight #11 on 19 April 2008 en route from/to California, because this study focuses on the Arctic region. In general, Hg° remained fairly constant below 4 km centered at ~170 ppqv followed by a decrease above 4 km; O_3 mixing ratios <50 ppbv were observed below 1 km altitude (Fig. 1). Near the surface Hg° and O_3 dropped frequently to near zero, and above 6 km, Hg° was depleted below 50 ppqv when O_3 levels exceeded 100 ppbv in stratospherically influenced air (Talbot et al. 2007). A total of 603 data points were obtained below 1 km altitude and north of 50°N, and 99% of the data showed O_3 levels <55 ppbv with an Hg°-O_3 linear correlation and r^2 value of 0.68 and a slope of 3.3 ppqv Hg°/ppbv O_3 (Fig. 2). Above 1 km there was no correlation between Hg° and O_3. The r^2 and slope values below 1 km altitude are close to those found in April-early June 1995 measurements at Alert by Schroeder et al. (1998). However, our values were obtained over a much larger geographic region at multiple altitudes below 1 km in the month of April providing a regional relationship between Hg° and O_3 in the springtime Arctic.

To provide a general picture, transects of Hg° and O_3 as well as corresponding aircraft altitudes from the nine flights in the spring deployment are shown in Fig. 3. Over the frozen open ocean the mixing ratio of Hg° was mostly in the range of 150–200 ppqv and O_3 50–75 ppbv. In a few incidences Hg° was observed to be less than 50 ppqv and O_3 less than 50 ppbv at altitudes below 2 km. Over Alaska Hg° mixing ratios were in the range of 100–200

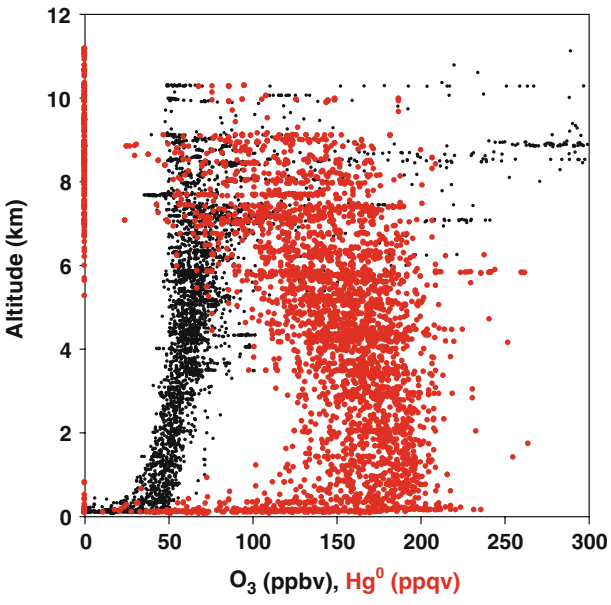

Fig. 1 Vertical distributions of Hg° (*red*) and O_3 (*black*) based on measurements from all springtime flights of ARCTAS excluding samples south of 50°N which were collected on Fight #1 on 1 April 2008 and Flight #11 on 19 April 2008 en route from/to California

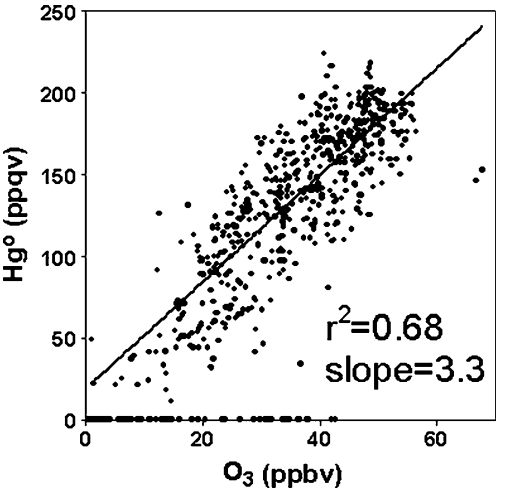

Fig. 2 Scatter plots of Hg° versus O_3 for all near surface data, which showed O_3 mixing ratios were all below 60 ppbv except 2 data points. The regression was fitted without Hg° below the LOD. Data with Hg° below the LOD are shown in this figure as Hg° = 0 pptv; they suggest that near zero Hg° events occurred at a variety of O_3 mixing ratios

ppqv and O_3 greater than 50 ppbv at altitude above 2 km, and over Canada the aircraft appeared to sample frequently high altitude air masses that were influenced by stratospheric air indicated by Hg° less than 50 ppqv and O_3 greater than 100 ppbv at altitudes above 6 km.

During the nine flights in the spring deployment, Hg° depletion was found during eight time periods accompanied by low or depleted O_3 levels near the surface along the northern Alaskan and Canadian coastlines as well as over the Arctic Ocean (Fig. 4). There was distinct variability in the vertical structure from day to day with a corresponding change in the height of the inversion, which is indicated by the potential temperature gradient >5 K in the discussion of individual cases below. The vertical and horizontal gradients of Hg° were on the order of 100 ppqv or more and these are 10 times greater than the precision of the Hg ° measurements. However, they are specific to the conditions present when the measurements were conducted. There is not enough data to make generalized statements and demonstrate consistent trends in Hg°. Thus, we present individual depletion events and summarize the characteristics of each one.

The vertical distributions of potential temperature and wind from those time periods differed largely indicating great variability in atmospheric dynamics. However, one common feature amongst all cases was the occurrence of an inversion layer near the surface, which effectively blocked air mixing downward from aloft. This situation resulted in noticeable depletion of trace gases near the surface owing to the predominance of loss mechanism(s) there. Moreover, vertical profiles of Hg°, O_3, and other trace gases were also quite different between cases. For instance, April 9, April 16, and April 18 cases appear to be more complex than the April 8 case, which is suggested by more structure in the vertical profiles of trace gases such as the change in the height of the inversion. Our focus was on the air below the inversion where the depletion events occurred. These events had consistent chemical characteristics of low Hg°, O_3, and selected light hydrocarbons.

April 8 In the 8 April case, Hg° decreased abruptly from 142 ppqv to below LOD and O_3 levels dropped from over 40 ppbv to single digits over 17:22–17:50 UT. This was the longest record of Hg° depletion captured in measurements during the entire spring deployment. A close examination of the 1 s data for the 30 min spiral preceding the depleted Hg° event revealed that a ~200 m thick boundary layer was isolated from the free troposphere by a second strong

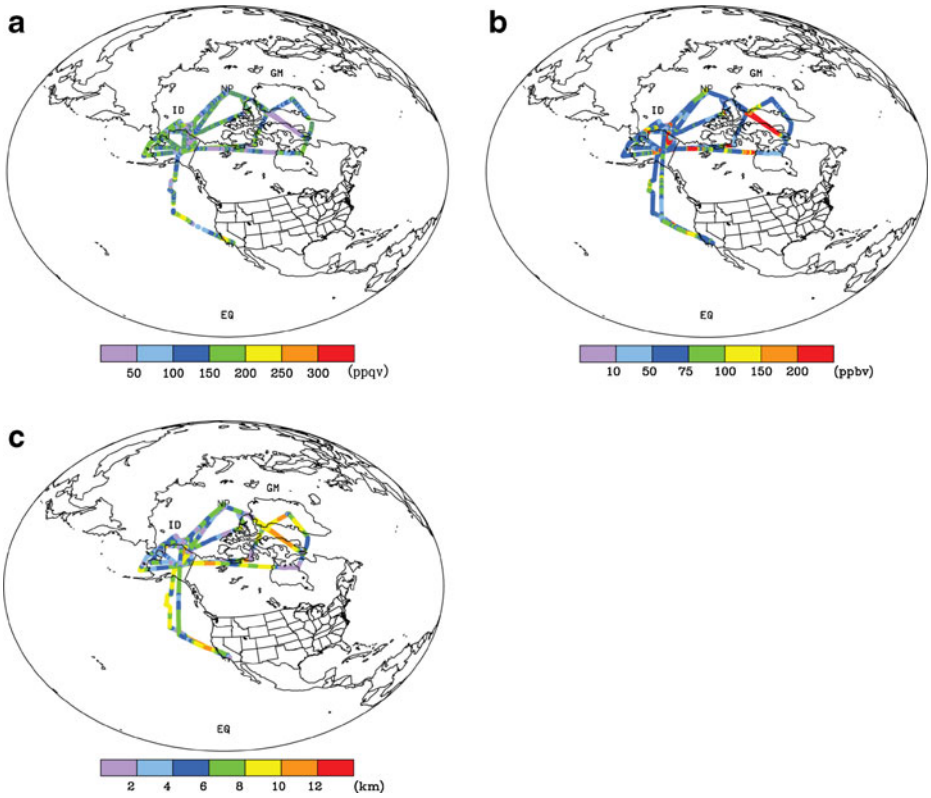

Fig. 3 Transects of (**a**) Hg°, (**b**) O_3, and (**c**) corresponding aircraft altitude from all nine flights of the spring deployment

inversion layer situated between 200 and 400 m altitude (Fig. 5a). In particular, the strongest point in the inversion layer appeared to be a potential temperature increase of ~10 K over a 15 m thickness at ~250 m altitude. A concomitant precipitous plummet of Hg° from 142 ppqv to zero was observed, accompanied by a steep decrease of 45 ppbv in O_3. Abrupt decreases in

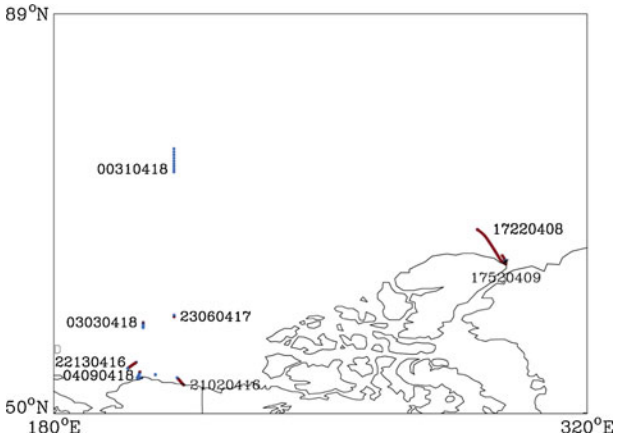

Fig. 4 Locations of Hg° <35 ppqv and corresponding O_3 levels (blue: 0–10 ppbv; burgundy: 10–50 ppbv). The numbers represent the time of the beginning of each AMDE in the form of hour, minute, month, and day each in 2 digits

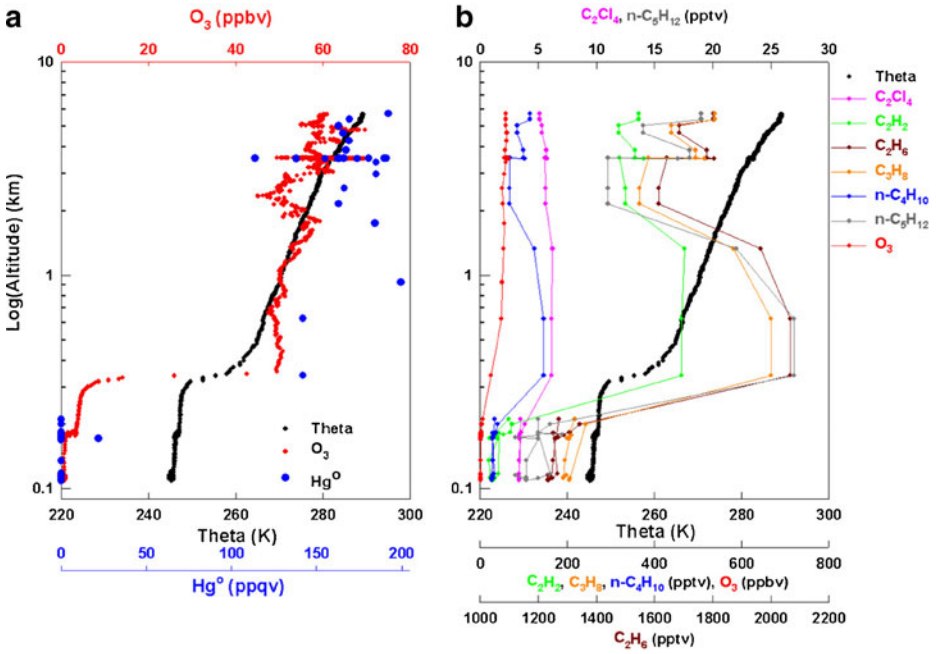

Fig. 5 Vertical profiles of 1-minute Hg°, 1-second O_3 and potential temperature (**a**) and 1-minute C_2Cl_4, C_2H_2, and alkanes, and O_3 (**b**) during time periods including the occurrence of depleted Hg°: 17:22–17:50 UT, 8 April, 2008

ethyne (C_2H_2), tetracholoroethene (C_2Cl_4), and alkanes across the inversion layer were also clearly visible in their vertical profiles (Fig. 5b). For example, C_2H_2 mixing ratios decreased from 462 pptv immediately above the inversion layer to 73 pptv right below it, C_2Cl_4 from 6.2 to 3.8 pptv, n-butane (n-C_4H_{10}) from 146 to 40 pptv, and n-pentane (n-C_5H_{12}) from 27 to 6 pptv. Apparently the loss mechanism(s) caused a considerable uniform loss of O_3, Hg°, C_2H_2, C_2Cl_4, and alkanes below ~200 m altitude, which resulted in steep vertical gradients in these compounds across the inversion layer.

The wind profile suggested wind speed and direction were highly variable during the hour the aircraft sampled Hg°-depleted air masses near the surface. Wind speed ranged over 5–10 m s^{-1} at the surface and over 10–12 m s^{-1} from the surface to 3 km. Clearly strong wind shear existed near the surface and thus turbulence was most likely occurring at the time, which facilitated consistent depletion of Hg° and O_3 at all altitudes below the inversion layer. The 5-day back trajectories for the Hg° depleted air masses indicated various possible origins with the majority between the surface and 860 hPa (Fig. 6a). The exception revealed that the air mass with zero Hg° could have come from altitudes as high as 660–700 hPa, indicating subsidence of free tropospheric air followed by depletion near the surface. The horizontal distance of Hg° depleted area covered by airborne measurements alone reached ~200 km. It is thus speculated that Hg° depletion likely occurred over a rather extensive area both horizontally and vertically.

Carbon monoxide (CO) and carbon dioxide (CO_2) were correlated at r^2=0.97 and a slope value of 0.1 ppbv CO/ppmv CO_2, close to the northeastern U.S. regional value of 0.08 ppbv CO/ppmv CO_2 (Potosnak et al. 1999; Mao and Talbot 2004). This together with the back trajectories in Fig. 6a indicate that air masses with such a strong anthropogenic signature might have originated mainly from northern and eastern Canada and Greenland.

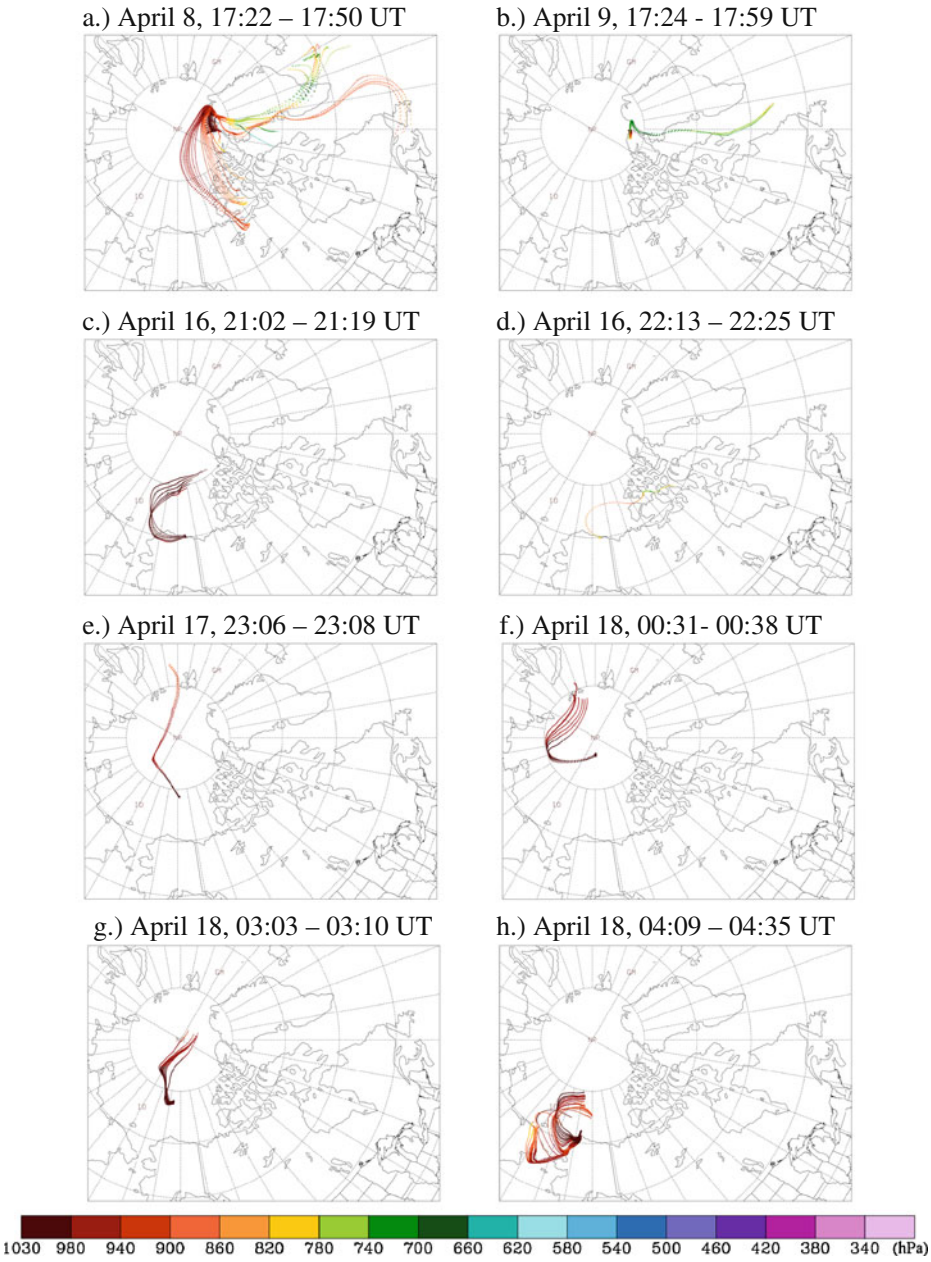

Fig. 6 Five-day back trajectories originated from the locations with depleted Hg° and O_3 levels for the eight Hg° depletion cases

April 9 On April 9, during the 35 min spiral from 17:24 to 17:59 UT including the depleted Hg° sampling at the surface over 17:52–17:54, two inversion layers were observed at altitudes of 1.2–1.6 km and 0.15–0.4 km with a potential temperature increase of 11 K and 5 K respectively (Fig. 7a). Inside and below the first inversion layer was there actually an

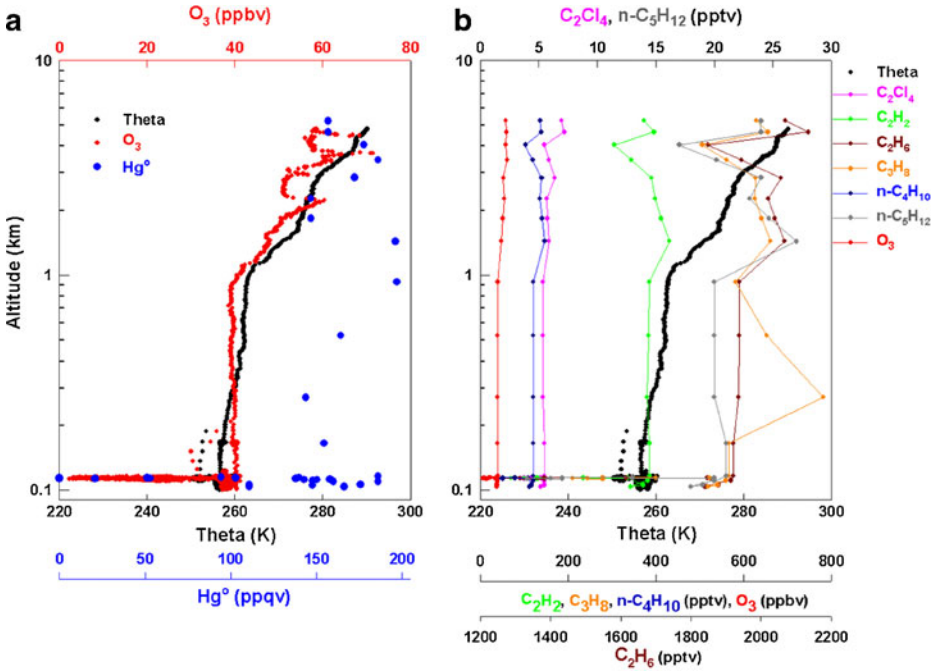

Fig. 7 Vertical profiles of 1-minute Hg°, 1-second O_3 and temperature (**a**) and 1-minute C_2Cl_4, C_2H_2, and alkanes, and O_3 (**b**) during time periods including the occurrence of depleted Hg°: 17:24–17:59 UT, April 9, 2008

increase in Hg° mixing ratios, whereas below the second inversion layer Hg° levels decreased. Depleted Hg° was observed at 17:52–17:54 UT near the surface corresponding to the lowest temperature (~ −22°C) portion of this transect. During the transect temperature ranged over −11 to −22°C, Hg° mixing ratios 0–186 ppqv, and O_3 levels 3–41 ppbv. This transect extended from the points of closest distance over the bay between Greenland and Ellesmere Island to north of Alert out over the Arctic Ocean.

Over this area there was a steep horizontal gradient in Hg° and O_3 mixing ratios in contrast to a rather gradual one in temperature. Hg° was around 186 ppqv at the narrowest point of the bay followed by decreases to 103 ppqv over a distance of ~120 km toward the frozen open ocean, and then over a distance of ~9 km Hg° plummeted to zero after the aircraft flew out of the strait reaching north of Alert. Along the coast of the frozen open ocean, Hg° mixing ratios rose to 124 ppqv over a horizontal distance of ~60 km. The distance of depleted Hg° levels was estimated to be~20 km. Close examination of this event indicates a highly heterogeneous distribution of Hg° mixing ratios with abrupt changes from the bay to coastal area, and furthermore, a depleted Hg° area on a spatial scale of a few tens of kilometers. Our data indicate that there are numerous “mercury holes” in the springtime Arctic coastal zone atmosphere.

Concurrent changes in C_2H_2, C_2Cl_4, and alkanes showed similar trends to those in Hg° and O_3 with the steepest decrease at the surface (Fig. 7b). These trace gases exhibited abrupt decreases of >50% corresponding to the precipitous fall of Hg° mixing ratios from 103 ppqv to zero, except C_2Cl_4 which experienced a 23% decrease possibly due to its slower reaction rate with Cl compared to other traces gases.

In the Hg°-depleted zone winds were nearly calm (<2 m s^{-1}), and the 5-day trajectories for the April 9 event suggested localized flow patterns (Fig. 6b), which implies that the Hg°

depletion may have occurred in a rather concentrated area as opposed to over an extended route as in the April 8 case. However, CO and CO_2 mixing ratios were found to be the highest at ~165 ppbv and ~392 ppmv respectively, albeit uncorrelated, concomitant with depleted Hg° and single digit levels of O_3. It should be noted that the CO_2 level measured in the Arctic was constantly >392 ppmv, compared to the 386 ppmv global background mixing ratio in 2008 (http://www.esrl.noaa.gov/gmd/ccgg/trends/). This implies a pervasive anthropogenic influence embedded in the background levels of trace gases in the springtime Arctic atmosphere.

April 16 During the April 16 deployment the aircraft sampled depleted Hg° at ~90–800 m altitudes during 21:02–21:19 UT and at ~90–500 m during 22:13–22:25 UT, on the Alaskan coast close to the Canadian border and ~400 km away in the near-coastal area over the Arctic Ocean (Fig. 4). One common feature in the vertical structure of potential temperature from the two time periods was the occurrence of two inversion layers, and depletion occurred below the lowest inversion layer (Fig. 8). During 21:02–21:19 UT the aircraft crossed the coastline descending over land followed by an ascent over the ocean. On land Hg° was found to be depleted at the 70 m altitude and above that altitude was >70 ppqv, whereas measurements over the frozen open ocean revealed that the Hg°-depleted layer extended up to ~900 m (Fig. 8a). During 22:13–22:25 UT on the descending leg measurements were over the ocean and showed that the lower inversion layer extended from ~500 m to the surface with a 5 K change in potential temperature, accompanied by depleted Hg° and O_3 mixing ratios <10 ppbv (Fig. 8c), while on the ascending leg the depletion extended to the ~500 m altitude accompanied by an inversion layer between 530 and 840 m with a ~5 K potential temperature increase. Correspondingly over 21:02–21:19 UT, C_2Cl_4, C_2H_2, and alkanes showed the same trend in their vertical distribution, lower near the surface and increased above (Fig. 8b), while over 22:13–22:25 UT these species showed lower mixing ratios throughout the Hg°-depleted/O_3-poor layer from the surface to ~900 m (Fig. 8d). This deployment demonstrates that over the frozen ocean the Hg°/O_3-poor layer appears to be much deeper than over land.

The 5-day back trajectories (Fig. 6c and d) indicated that air masses at the Hg°-depleted locations, be it on the Canadian coast or over the frozen ocean surface, had been circulating over the Arctic Ocean in their recent history. The Hg°, O_3 and VOC loss mechanisms again appear to be pervasive over the Arctic Ocean and its adjacent area. The horizontal distance covered by Hg° depletion in the two time periods was estimated to be 120–140 km.

April 17–18 On the April 17–18 flight the aircraft sampled Hg°-depleted air masses four times: 1.) 23:06–23:08 (Fig. 9a and b), 2.) 00:31–00:38 (Fig. 9c and d), 3.) 03:03–03:10 (Figs. 9e, f and 4.) 04:09–04:35 UT (Fig. 9g and h). The first three cases were in the middle of the Arctic Ocean and the fourth one was near- and on the Alaskan coast (Fig. 4). The first, third and fourth cases (Fig. 9a, e and g) had similar structure in the inversion layer, an increase >5 K in potential temperature within the 150–200 m layer and relatively weak winds with its speed varying from 2 to 6 m s^{-1}. In these three cases, near the surface the mixing ratio of Hg° was mostly zero, or of a few tens of ppqv accompanied by either zero or very low O_3 mixing ratios (Fig. 9b, f and h), and correspondingly the mixing ratios of C_2Cl_4, C_2H_2 and alkanes showed similar trends. The second case (Fig. 8c) differed in its instability below 200 m as evidenced by constant potential temperature indicative of a well-mixed layer. In this case, we showed a descending leg from 5 km to the surface followed by an ascending one from the surface to 1 km. On the descending leg, an inversion layer occurred between 400 m and 900 m altitude indicated by a 6 K potential temperature

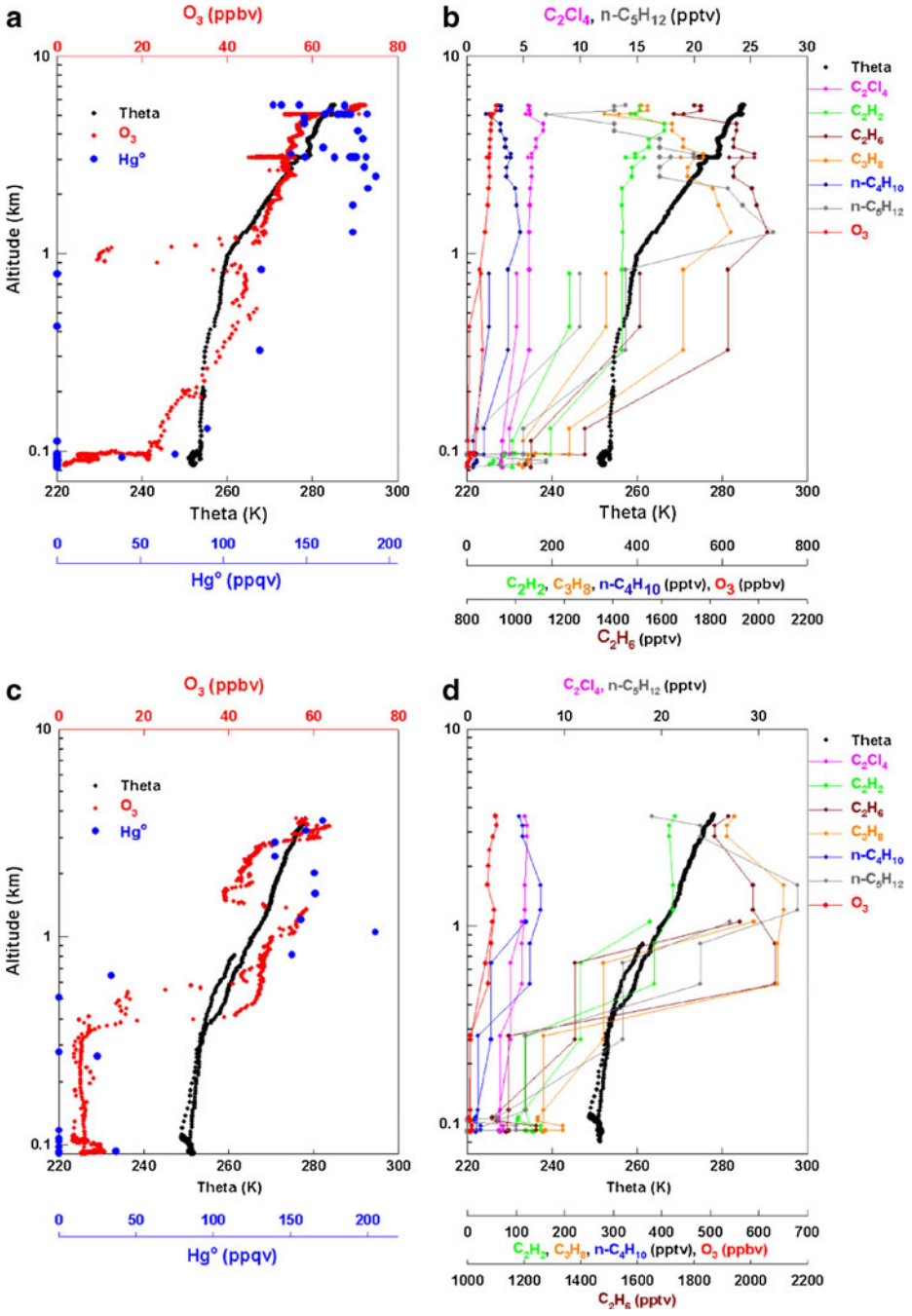

Fig. 8 Vertical profiles of 1-minute Hg°, 1-second O_3 and temperature (**a**, **c**) and 1-minute C_2Cl_4, C_2H_2, and alkanes, and O_3 (**b**, **d**) during time periods including the occurrence of depleted Hg°: 21:00–21:19 (**a**,**b**) and 22:13–22:25 (**c**,**d**), April 16, 2008

Fig. 9 Vertical profiles of 1-minute Hg°, 1-second O_3 and temperature (**a**, **c**, **e**, and **g**) and 1-minute C_2Cl_4, C_2H_2, and alkanes, and O_3 (**b**, **d**, **f**, and **h**) during time periods including the occurrence of depleted Hg°: 22:50–23:08 April 17 (**a**,**b**), 23:52 April 17–00:38 April 18 (**c**,**d**), 02:52–03:10 April 18 (**e**,**f**), 04:00–04:35 April 18, 2008 (**g**,**h**)

gradient, and below the 400 m altitude depletion of Hg°, O_3, C_2Cl_4, C_2H_2 and alkanes was observed. On the ascending leg, a strong inversion occurred between 300 m–900 m altitude marked by a ~12 K increase in potential temperature, and depletion of trace gases extended to an altitude of 800 m.

It should be noted that in the fourth case, variability in potential temperature, Hg°, O_3, and other trace gases was observed near the surface (Fig. 8g and h), e.g., Hg° increasing from 0 to 44 ppqv accompanied by potential temperature from 251.8 K to 253.3 K. Based on the location of the aircraft indicated in Fig. 4 and the time series of longitude/latitude/altitude (not shown), such variability occurred when the aircraft was flying eastward along the Alaskan coast.

The 5-day backward trajectories for the four time periods suggested that Hg°-depleted air masses had been circulating over the Arctic Ocean or over land near the coast (Fig. 6e, f, g and h). It should be pointed out that the four Hg°-depletion cases were captured in spiral measurements whenever the aircraft flew low. Therefore, even though it is impossible to speculate whether there was horizontal continuity in Hg° depletion, our analysis illustrates the pervasiveness and persistence of zero or very low levels of Hg° and O_3 near the surface of the Arctic Ocean.

4 Linkage between AMDE/ODE and halogens

4.1 Relationships between Hg°, O_3 and VOCs

Relationships between Hg° and a suite of trace gases measured north of 50°N were examined during all eight AMDEs and ODEs. Hg° and O_3 were found to be correlated with C_2Cl_4 at r^2= 0.68 and 0.81 respectively, excluding the points of Hg°<LOD (Fig. 10a and b). Tetrachloroethylene is an industrial solvent, a useful indicator of anthropogenic influence, with a lifetime of ~5 months. The reaction of C_2Cl_4 with Cl is 6 orders of magnitude faster than with Br (Ariya et al. 1997), and thus Cl is considered to be the dominant oxidant for C_2Cl_4.

As described in the previous section, C_2Cl_4, C_2H_2, and alkanes also decreased to low mixing ratios accompanying depleted Hg° and O_3. It should be noted that data points from 21:42 and 21:45 UT on April 17 were excluded since these measurements seemed to be contaminated by a fresh plume based on ethane (C_2H_6), propane (C_3H_8), n-butane (n-C_4H_{10}), n-pentane (n-C_5H_{12}), n-hexane (n-C_6H_{12}) and levels being higher than the neighboring data by a factor of 4–10. Correlation was found for C_2Cl_4 with C_2H_2, C_2H_6, C_3H_8, n-C_4H_{10}, and n-C_5H_{12} near the surface (<1 km) with r^2 values in the range of 0.43–0.84 (Fig. 10c, d, e, f and g; Table 1). The depleted fraction of C_2Cl_4, C_2H_2, and alkanes was defined as the ratio of the depleted to the background level. It was found that the natural logarithmic value of the depleted fraction of C_2Cl_4 and alkanes was linearly correlated with the rate constants of their reactions with Cl (Fig. 11), in agreement with previous studies (Jobson et al. 1994; Ariya et al. 1999). This clearly suggests the predominant role of Cl in oxidation of C_2Cl_4 and alkanes in the near surface atmosphere of the springtime Arctic.

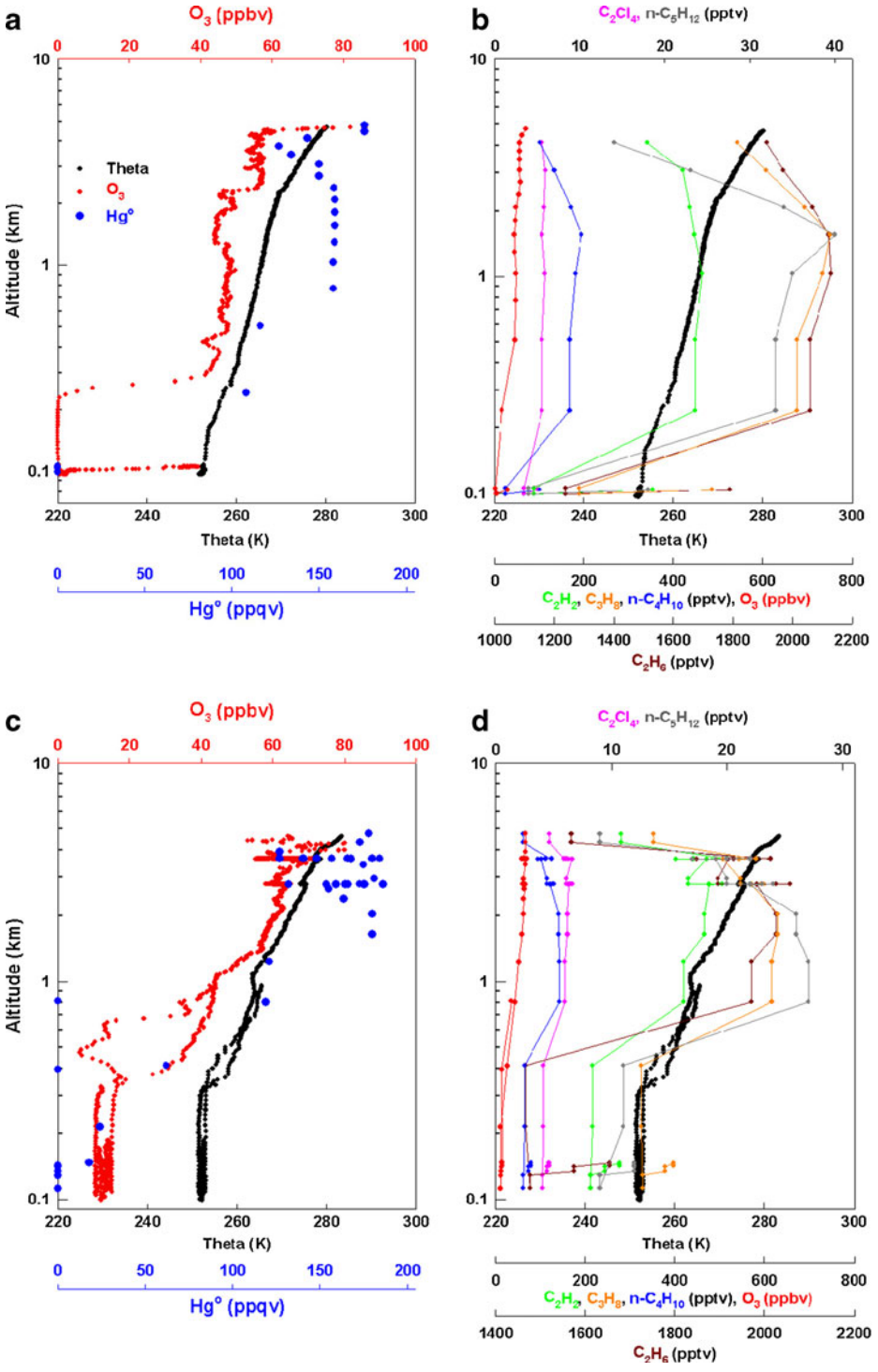
a
O3 (ppbv)
0 20 40 60 80 100
10
1
0.1
Altitude (km)
Theta
O3
Hg°
220 240 260 280 300
Theta (K)
0 50 100 150 200
Hg° (ppqv)
b
C2Cl4, n-C5H12 (pptv)
0 10 20 30 40
10
1
0.1
220 240 260 280 300
Theta (K)
0 200 400 600 800
C2H2, C3H8, n-C4H10 (pptv), O3 (ppbv)
1000 1200 1400 1600 1800 2000 2200
C2H6 (pptv)
c
O3 (ppbv)
0 20 40 60 80 100
10
1
0.1
Altitude (km)
220 240 260 280 300
Theta (K)
0 50 100 150 200
Hg° (ppqv)
d
C2Cl4, n-C5H12 (pptv)
0 10 20 30
10
1
0.1
220 240 260 280 300
Theta (K)
0 200 400 600 800
C2H2, C3H8, n-C4H10 (pptv), O3 (ppbv)
1400 1600 1800 2000 2200
C2H6 (pptv)

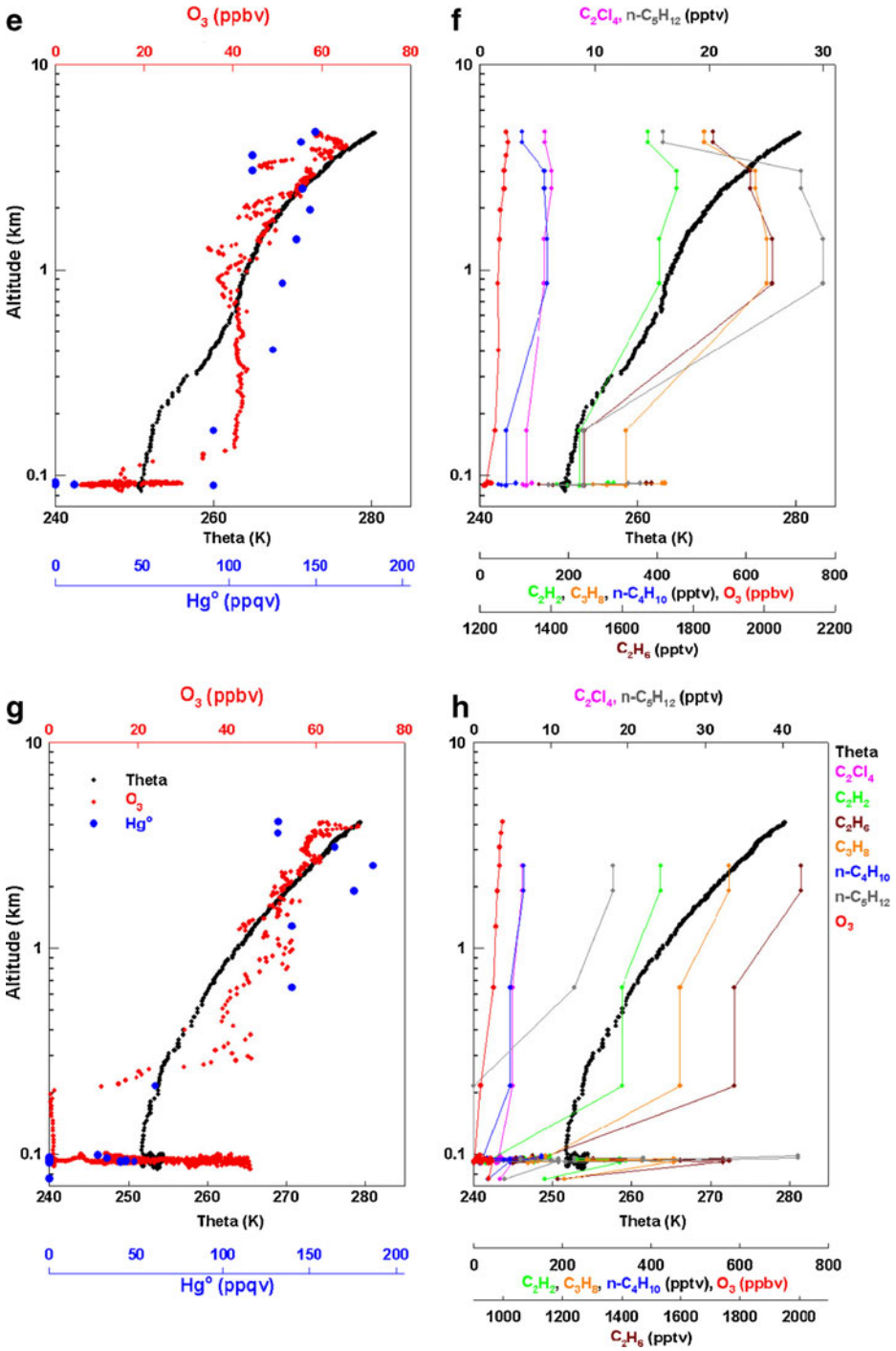

Fig. 9 (continued)

One exception is C_2H_2 which showed the largest deviation from the aforementioned linear correlation due to its fast oxidation by Br in the Arctic spring (Jobson et al. 1994; Ariya et al. 1999). The roles of Br and Cl are substantiated by the lack of a C_2H_2-CO correlation (not shown). We note that C_2H_2 and CO are often highly correlated in the troposphere owing to their common combustion source. During ARCTAS the lack of C_2H_2-CO correlation near the surface is signified by oxidative reactions of C_2H_2.

These findings are corroborated by the spring Arctic measurements from the Tropospheric Ozone Production about the Spring Equinox (TOPSE) airborne campaign conducted in winter/spring 2000 (Ridley et al. 2003). To be consistent, we used the measurements during the time period of April 4–18 2000 from TOPSE for comparison. We found r^2 and slope values from TOPSE close to the ARCTAS study for the C_2Cl_4-O_3, C_2Cl_4-C_2H_2, and C_2Cl_4-alkanes correlations (Fig. 12; Table 1) except C_2Cl_4-C_3H_8. It should be noted that there were 9 flights in ARCTAS compared to 3 in TOPSE over April 4–18, and under the criteria of latitude >50°N and altitude <1 km, there were 214 and 58 samples from ARCTAS and TOPSE respectively. Hence small differences in r^2 and slope values between the two campaigns can in part stem from the large discrepancy in sample size. Nonetheless, the close agreement in most cases adds rigor to our ARCTAS results (Fig. 13).

It should be pointed out that there were 27 data points (out of a total of 214 samples) with n-C_4H_{10} exceeding 210 pptv in the ARCTAS measurements. For that group of data the slope value of the C_2Cl_4 vs. n-C_4H_{10} correlation appeared to be different from the one at n-C_4H_{10} <210 pptv. The corresponding Hg° mixing ratios ranged from 110 to 215 ppqv with the median value of 186 ppqv, and O_3 from 41 to 55 ppbv with the median value of 48 ppbv. For n-pentane greater than 50 pptv, there were 16 points, and similar to the case of n-C_4H_{10}, the C_2Cl_4 vs. n-C_5H_{12} correlation appeared to be in a different regime with a larger slope value and Hg° and O_3 median values of background mixing ratios. These results may imply that the ratio of the oxidation rates of C_2Cl_4 and n-C_4H_{10} (or n-C_5H_{12}) increased when mixing ratios of n-C_4H_{10} and n-C_5H_{12} exceeded certain levels; but it is not clear what exactly was driving this. However our results are still valid because: 1) our equations were derived for Hg° and O_3 depletion events, while the Hg° and O_3 mixing ratios corresponding to the higher n-C_4H_{10} and n-C_5H_{12} regimes shown in Fig. 10 were far from AMDEs and ODEs; 2) the relationships of C_2Cl_4 vs. n-C_4H_{10} and C_2Cl_4 vs. n-C_5H_{12} were not used in our derivation.

4.2 Depletion rates of Hg° and O_3

The depletion rate (D) of O_3 or Hg° is the summation of reaction rates from reactions between Hg° or O_3 and halogen radicals:

$$D = \frac{d[X]}{dt} = \sum_{j=1}^{M} k_j[C_j][X] = [X]\sum_{j=1}^{M} k_j[C_j] \tag{1}$$

where X represents Hg° or O_3, C_j the concentration of halogen radical j, k_j the reaction rate constant of the reaction between X and C_j, and M the total number of reactions. This equation can be written in the form of

$$D = f[X] \tag{2}$$

where $f = \sum_{j=1}^{M} k_j[C_j]$. We define f to be the depletion rate coefficient in units of s^{-1}.

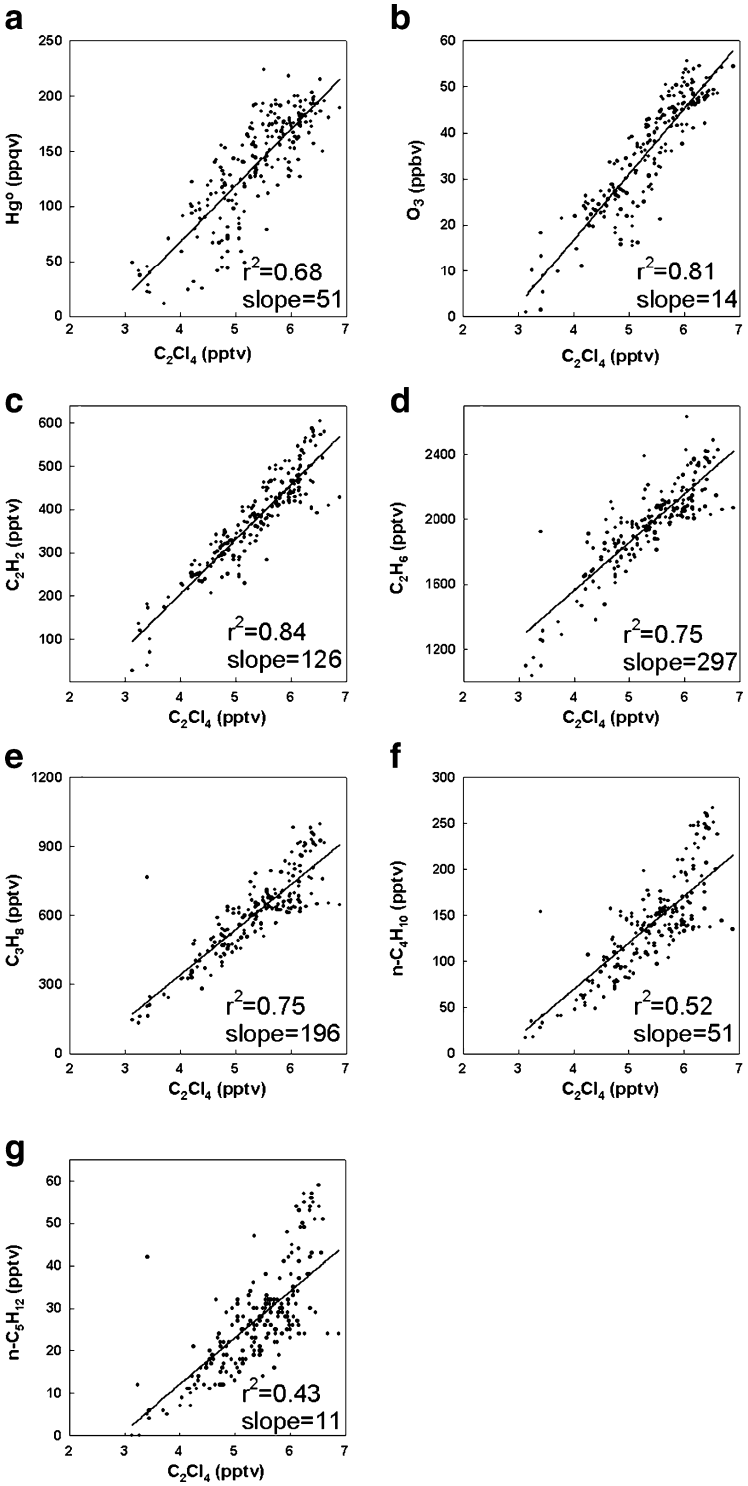
a
Hg° (ppqv)
C2Cl4 (pptv)
r2=0.68
slope=51
b
O3 (ppbv)
C2Cl4 (pptv)
r2=0.81
slope=14
c
C2H2 (pptv)
C2Cl4 (pptv)
r2=0.84
slope=126
d
C2H6 (pptv)
C2Cl4 (pptv)
r2=0.75
slope=297
e
C3H8 (pptv)
C2Cl4 (pptv)
r2=0.75
slope=196
f
n-C4H10 (pptv)
C2Cl4 (pptv)
r2=0.52
slope=51
g
n-C5H12 (pptv)
C2Cl4 (pptv)
r2=0.43
slope=11

Fig. 10 Correlation of C_2Cl_4 with Hg°, O_3, C_2H_2, and several alkanes from ARCTAS measurements for all sample points, which occurred below 1 km altitude and north of 50°N. Points of Hg°<LOD and corresponding C_2Cl_4, O_3, C_2H_2, and alkanes were excluded

Assuming the only loss mechanism for C_2Cl_4 is reaction with Cl and using the C_2Cl_4-O_3 and Hg°-O_3 correlations, we derived order-of-magnitude estimates of f from the DC-8 observational data as a function of the Cl concentration for samples with Hg° exceeding the LOD during AMDEs:

$$f_{Hg^\circ} = \sum_{i=1}^{N} k_{Hg^\circ - C_i}[C_i] \quad \sim 10^{-10}[Cl] \tag{3}$$

$$f_{o_3} = \sum_{j=1}^{M} k_{o_3 - C_j}[C_j] \quad \sim 10^{-10}[Cl] \tag{4}$$

for the average air temperature of 254 K during ARCTAS, where $k_{Hg^o - C_i}$ represents the rate constant for the reaction between Hg° and halogen radical i, $k_{O_3 - C_j}$ the rate constant for the reaction between O_3 and halogen radical j, $[C_i]$ and $[C_j]$ the concentration of halogen radicals i and j, respectively, $[Cl]$ the concentration of Cl, M and N the number of reactions of Hg° and O_3, respectively, with halogen radicals. The detailed derivation of Eqs. (3) and (4) can be found in the Appendix. As shown in the Appendix, we expressed d[Hg°]/dt and d[O_3]/dt as a function of other chemical species (e.g., C_2Cl_4) and used the values of the slopes from these relationships. After substitution into the expressions, the depletion rates are shown to be approximated as a function of the [Cl]. The reaction rate constant for C_2Cl_4 with Cl was obtained from Thuner et al. (1999).

Two points should be noted here. First, relationships expressed in Eqs. 3 and 4 do not imply that Cl chemistry is primarily responsible for AMDEs and ODEs. Instead, these relationships between the Hg° (and O_3) depletion rate and Cl levels represent the net outcome of complex and largely unknown mechanisms causing springtime Arctic Hg° and O_3 depletion. Second, these equations do not apply to Hg° depleted to below LOD. As shown in the Appendix, in deriving Eqs. (3) and (4) we used the ratio [C_2Cl_4]/[Hg°]. Clearly for Hg°<LOD, this ratio would approach infinity. For those samples, O_3 mixing ratios varied from below LOD to 42 ppbv. This implies that the chemistry driving completely depleted Hg° levels is likely very different from the concurrent one that involves O_3.

Table 1 The r^2 and slope values (in unit of ppqv/pptv for Hg°, ppbv/pptv for O_3 and pptv/pptv for the remaining species) of correlation of C_2Cl_4 with Hg° (not available in TOPSE), O_3, C_2H_2 and several alkanes from ARCTAS and TOPSE measurements. There were 9 flights in ARCTAS compared to 3 in TOPSE during the time period of April 4–18, and under the criteria of O_3 <50 ppbv, latitude >50°N, altitude <1 km, and points of Hg°<LOD excluded, there were 191 and 57 samples from ARCTAS and TOPSE respectively

	Hg°		O_3		C_2H_2		C_2H_6		C_3H_8		n-C_4H_{10}		n-C_5H_{12}	
ARCTAS	.68	51	.81	14	.84	126	.75	297	.75	196	.52	51	.43	11
TOPSE			.77	13	.82	158	.49	234	.74	150	.67	52	.57	10

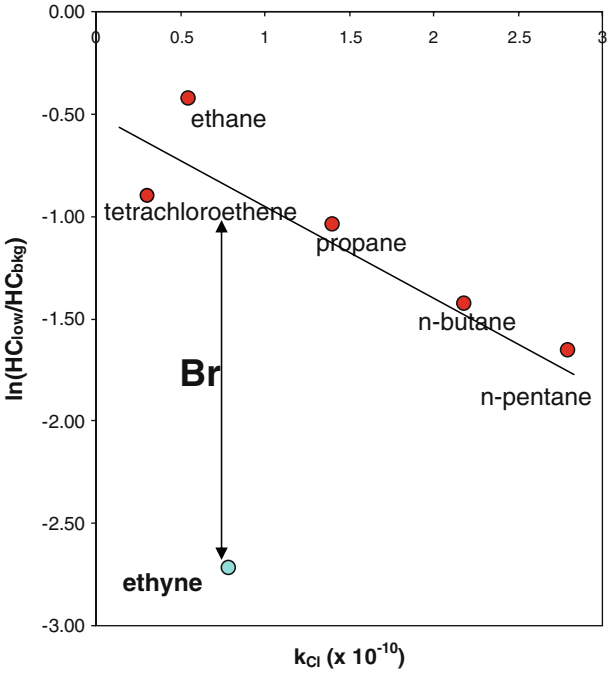

Fig. 11 Natural logrithmic values of the ratio of the depleted to background level of trace gases versus rate constants of their reactions with Cl for the Hg° depletion case on April 8, 2008

Furthermore, considering C_2H_2 is primarily oxidized by OH, Cl, and Br, we can express the rate of C_2H_2 oxidation as

$$\frac{d[C_2H_2]}{dt} = -\left(k_{OH-C_2H_2}[OH] + k_{Cl-C_2H_2}[Cl] + k_{Br-C_2H_2}[Br]\right)[C_2H_2] \tag{5}$$

for an average air temperature of 254 K (i.e. the average temperature near the surface in the AMDE/ODE zones during ARCTAS), where $k_{x\text{-}C2H2}$ represents the rate constants for the reactions of C_2H_2 and radical X (e.g., X = Cl, Br, or OH). We used the reaction rate constants for reactions of C_2H_2 with OH and Cl from Sander et al. (2002) and that for C_2H_2 with Br from Atkinson et al. (2006). We combined the Hg°-C_2H_2 (r^2=0.70 and a slope value of 0.38 ppqv/pptv) and O_3-C_2H_2 (r^2=0.80 and a slope value of 0.1 ppbv/pptv) correlations (Fig. 12) with Eq. 5, and expressed the Hg° and O_3 depletion rate coefficients as a function of OH, Cl, and Br concentrations as order-of-magnitude estimates:

$$f_{Hg^\circ} = \sum_{i=1}^{N} k_{Hg^\circ-C_i}[C_i] \qquad \sim 10^{-13}[OH] + 10^{-10}[Cl] + 10^{-14}[Br] \tag{6}$$

$$f_{0_3} = \sum_{j=1}^{M} k_{0_3-C_j}[C_j] \qquad \sim 10^{-13}[OH] + 10^{-10}[Cl] + 10^{-14}[Br] \tag{7}$$

The detailed derivation of Eqs. (6) and (7) can be found in the Appendix. Note that these relationships (i.e., Eqs. 3, 4, 6, and 7) were derived from the actual DC-8 in situ measurements rather than from theoretical analysis. Again note that Eqs. (6) and (7) do not apply to data where Hg°<LOD.

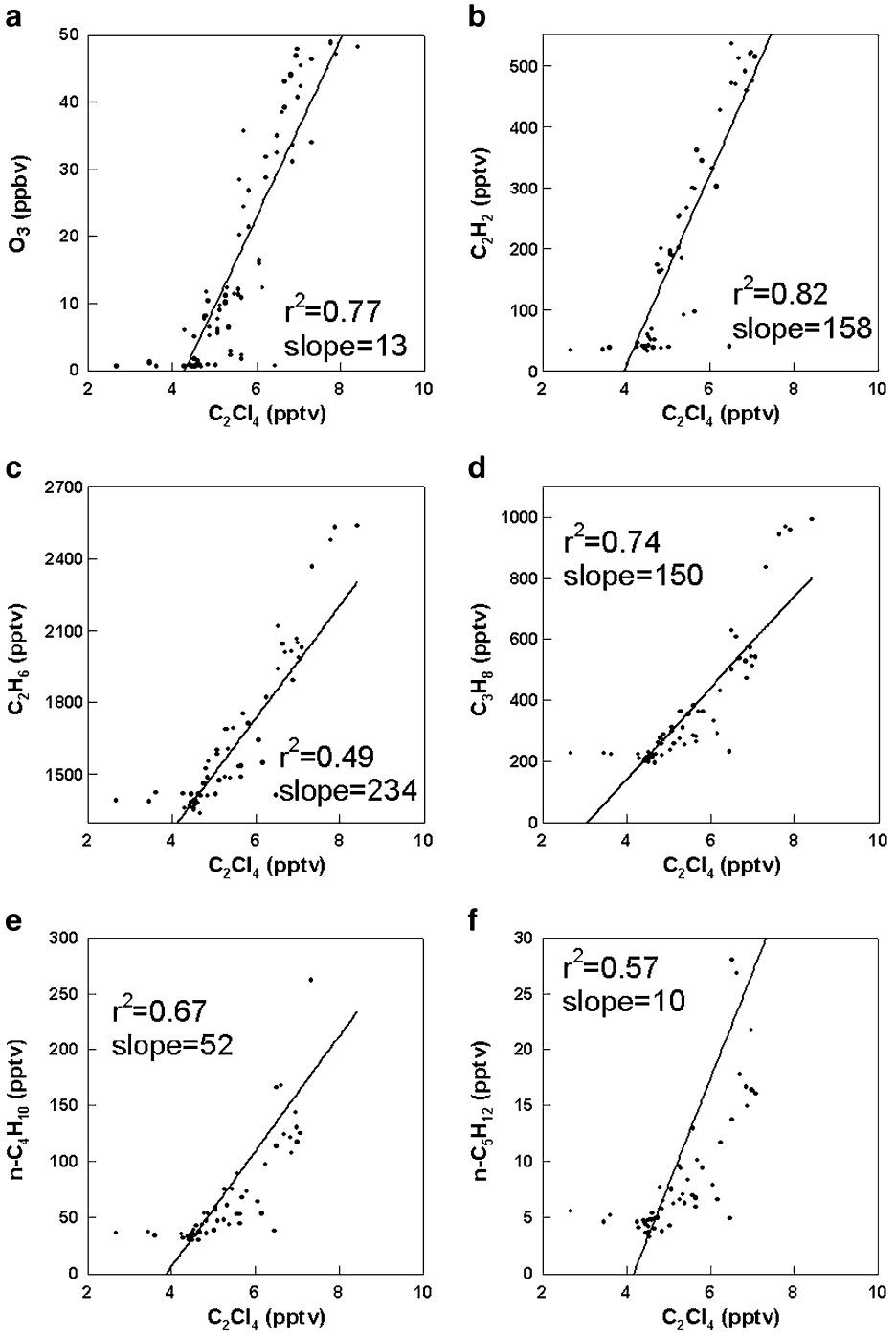

Fig. 12 Correlation of C_2Cl_4 with O_3, C_2H_2, and several alkanes from TOPSE measurements for all sample points, which occurred below 1 km altitude and north of 50°N

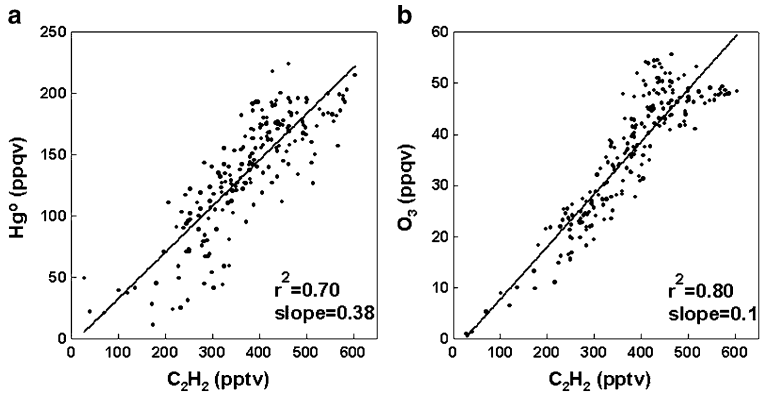

Fig. 13 Correlation of C_2H_2 with Hg° and O_3 from ARCTAS measurements for all sample points, which occurred below 1 km altitude and north of 50°N. All sample points with Hg°<LOD and corresponging C_2H_2 and O_3 were excluded

4.3 Examples for application of derived equations

To illustrate the potential application of the equations derived here, we obtained order-of-magnitude estimates of the ratio [Br]/[Cl] using use Eqs. (6) and (7). Since ground-based measurements were not available during ARCTAS, we used the depletion rate of O_3 and Hg° from Sprovieri et al. (2005), where O_3 decreased from 45 ppbv to 10 ppbv and Hg° from 1.6 ng m^{-3} to 0.6 ng m^{-3} (i.e., from 179 to 67 ppqv) within 24 h in the spring Arctic. These depletion rates are similar to those obtained by Kim et al. (2010) in a box model study of the ARCTAS mercury depletion. However, it should be cautioned that the depletion rates of O_3 and Hg° concurrent to the ARCTAS deployment might be different from the values from Sprovieri et al. (2005), which may induce uncertainties in the final estimates. The values of f_{O_3} and f_{Hg^o} are thus on the order of 10^{-5} s^{-1} respectively $\left(f_{O_3} = 1/[O_3] \times d[O_3]/dt, \text{similar for } f_{Hg^o}\right)$. On the right hand side of Eqs. 6 and 7, using [OH] = 3.6×10^5 molecules cm^{-3} (Kim et al. 2010), the OH oxidation term is on the order of 10^{-8} s^{-1}, which is negligible compared to the 10^{-5} s^{-1} order of magnitude for f_{O_3} and f_{Hg^o}. Even if we assume the Br and Cl terms were of the same order of magnitude, the ratio [Br]/[Cl] would need to be ~10^4 for the equation to hold valid. However, if the Br effect is a lot more significant as suggested by the literature, the ratio [Br]/[Cl] would be greater than 10^4.

The ratio [Br]/[Cl] derived here is close to the upper limit of the result in Sive et al. (2000) where the ratio varied from 10^3 to 10^4 from TOPSE for an assumption of 1–10 days of VOCs exposure to Br and Cl radicals. As has been documented in the literature, the ratio [Br]/[Cl] was derived using the slope value of $\ln[VOCs]_{depleted}/\ln[VOCs]_{background}$ versus the rate constants of the reactions of VOCs with Cl, and the C_2H_2 concentrations. The slope value varies depending on the depleted and background levels of VOCs, the number of VOCs considered, and the length of time of exposure to halogen radicals. Cavender et al. (2008) applied a 0-D photochemistry model and obtained the ratio [Br]/[Cl] ranging from ~100 to ~2000 for ODEs in the Arctic. In comparison, our ratio here is entirely derived from extensive observations, and we used the data with minimal assumptions to arrive at the expressions in Eqs. 3, 4, 6 and 7. Further, since our ratio is based on all measurements from the campaign, which spanned a month during ARCTAS, our ratio value should be fairly representative of the Arctic basin. Possible discrepancies between published values and our findings could be caused by many factors which are beyond the scope of this

work to evaluate. As more papers are published on Arctic tropospheric chemistry, hopefully there will be closure on many issues.

One of the most frequently discussed questions is how to identify contributions from in-situ and long-range distance transport to an observed depletion event. In the end of Section 3 we pointed out that, based on backward trajectories, Hg°-depleted air masses had been circulating over the Arctic Ocean or over land near the coast during the five days prior to the depletion events. Considering the four events that were captured at distantly spaced locations over the Arctic Ocean and its extended coastlines at different times of a month, we argue that an MDE or an ODE, at least the ones captured in our springtime ARCTAS measurements, is the net result of continual occurrence of depletion reactions in transit of air masses. Indeed, box model calculations for these MDEs by Kim et al. (2010) support this contention. Since the backward trajectories appeared to be confined in the Arctic region near the surface, it would be reasonable to hypothesize Hg° and O_3 depletion is driven by their reactions with halogen radicals. Therefore, the quantitative relationship between the depletion rate of Hg° (or O_3) and halogen radicals derived in this study reflect the total effect of those continual, in situ in a Lagrangian sense, oxidation reactions in the Arctic spring.

5 Summary

In this study we examined the vertical distributions of Hg° and O_3 together with C_2Cl_4, C_2H_2, and alkanes when Hg°- and O_3-depleted air masses were sampled near the surface (<1 km) utilizing measurements onboard the NASA DC-8 research aircraft during ARCTAS in April 2008 primarily over the North American Arctic. Our findings suggest that Hg° and O_3 depletion occurs from the surface up to 1 km altitude and covers linear distances ~20–200 km. Horizontally there was a sharp decreasing gradient of ~100 ppqv in Hg° over a <10 km distance from bay areas to the frozen open ocean. There was a distinct land-ocean difference in the vertical thickness of the Hg°-depleted layer – being variable but typically a few 100 meters over the ocean whereas occurring only near the surface over land. Based on multi-tracer relationships, we present expressions of the rates of Hg° and O_3 depletions as a function of radical concentrations.

There are three important implications from these expressions. First, the correlative relationships between Hg°, O_3, C_2Cl_4, C_2H_2, and alkanes provide observational evidence supporting that AMDEs are driven by Hg° reactions with halogen radicals. Second, in spite of the complex chemical reactions involved during AMDEs and ODEs, of which we still have a nebulous understanding, the depletion rates of Hg° and O_3 can be expressed as a function of Br, Cl, and OH concentration. Third, this analysis provides a useful metric for evaluation of models that attempt to reproduce Hg° and/or O_3 depletion events in the Arctic as well as providing a way to estimate the ratio [Br]/[Cl] with minimal assumptions.

Acknowledgments We thank the flight crew of the NASA DC-8 aircraft for their help with this field deployment and another successful airborne sciences mission. This work was supported by the NASA Tropospheric Chemistry Program under grant #NNG06GA56G and the NOAA AIRMAP grant #NA06OAR4600189 to UNH. We thank D. Jacob for useful discussions. We appreciate the two anonymous reviewers' constructive comments which helped clarify many points and improve the presentation of our work.

Appendix

Below is the derivation of Eqs. 1, 2, 4 and 5 for AMDEs and ODEs. Note that these expressions are used to obtain order-of-magnitude estimates of the radical concentrations.

The depletion rate of Hg° can be expressed as

$$\frac{d[Hg^{\circ}]}{dt} = \frac{d[Hg^{\circ}]}{d[C_2Cl_4]} \times \frac{d[C_2Cl_4]}{dt} \tag{1}$$

where $\frac{d[Hg^o]}{d[C_2Cl_4]}$ is approximated to be the discreet form $\frac{\Delta[Hg^o]}{\Delta[C_2Cl_4]}$, which is the slope value (51 ppqv/pptv) between these two species. Note: since the units of this slope value will be canceled by the units of C_2Cl_4/Hg° in (5), we do not need to convert the unit ppqv/pptv to molecules m^{-3}/molecules m^{-3} here; similarly, no unit conversion is needed for (8), (14), and (20), of the Hg°-C_2Cl_4 linear correlation (Fig. 9a in the manuscript), and $\frac{d[C_2Cl_4]}{dt}$ is expressed as:

$$\frac{d[C_2Cl_4]}{dt} = -k_{C_2Cl_4-Cl}[Cl][C_2Cl_4] \tag{2}$$

where $k_{C_2Cl_4-Cl}$ is the reaction rate constant for the reaction of C_2Cl_4 with Cl, and C_i represents radical species i. As stated in the manuscript, we used the value from Thuner et al. (1999) of 4.8×10^{-11} cm^3 $molecule^{-1}$ s^{-1} at 254 K. Therefore Eq. (1) can be expressed as:

$$\frac{d[Hg^o]}{dt} = -51 \times 4.8 \times 10^{-11}[Cl][C_2Cl_4] \tag{3}$$

The depletion rate can also be expressed as the summation of rates of all Hg° oxidation reactions (reaction i from 1 to the Nth reaction) as follows:

$$\frac{d[Hg^o]}{dt} = -\sum_{i=1}^{N} k_i[Hg^o][C_i] = -[Hg^o]\sum_{i=1}^{N} k_i[C_i] \tag{4}$$

Combining (3) and (4), we obtain

$$\sum_{i=1}^{N} k_i[C_i] = 51 \times 4.8 \times 10^{-11} \times \frac{[C_2Cl_4]}{[Hg^o]} \times [Cl] \tag{5}$$

In the manuscript, $\sum_{i=1}^{N} k_i[C_i]$ was defined as the depletion rate coefficient for Hg°. Based on the linear relation between Hg° and C_2Cl_4 excluding the Hg° mixing ratios below the LOD which are not part of the linear relationship (Fig. 10a in the manuscript):

$$[Hg^{\circ}] = -136 + 51 \times [C_2Cl_4] \tag{6}$$

In Fig. 10a, corresponding to 7% of the total samples where C_2Cl_4<3.34 pptv, the ratio $[C_2Cl_4]$/[Hg°] was in the range of 0.10–0.14 and to the remaining 93% of the data the ratio was on the order of the magnitude of 10^{-2}. In Scale Analysis, one uses orders-of-magnitude that is representative, not necessarily including every single point. Thus the ratio of C_2Cl_4/Hg° on the order of 10^{-2} was applied here. Same rationalization was applied in obtaining

other ratios in deriving Eqs. 13, 19 and 24. Using this ratio value for (5), we obtained the depletion rate coefficient of Hg° as follows:

$$\sum_{i=1}^{N} k_i[C_i] \sim 10^{-10} \times [Cl] \tag{7}$$

which is Eq.(2) in the manuscript.

The depletion rate of O_3 can be expressed as:

$$\frac{d[O_3]}{dt} = \frac{d[O_3]}{d[C_2Cl_4]} \times \frac{d[C_2Cl_4]}{dt} \tag{8}$$

Where $\frac{d[O_3]}{d[C_2Cl_4]}$ is approximated to be the discreet form $\frac{\Delta[O_3]}{\Delta[C_2Cl_4]}$, which is the slope value (14 ppbv/pptv) of the O_3-C_2Cl_4 linear correlation (Fig. 9b in the manuscript). Using this slope value together with Eq. (2), Eq. (8) can be expressed as:

$$\frac{d[O_3]}{dt} = -14 \times 4.8 \times 10^{-11}[Cl][C_2Cl_4] \tag{9}$$

The depletion rate of O_3 can also be expressed as the summation of rates of all O_3 oxidation reactions (reaction j from 1 to the Mth reaction) as follows:

$$\frac{d[O_3]}{dt} = -\sum_{j=1}^{M} k_j[O_3]\left[C_j\right] = -[O_3]\sum_{j=1}^{M} k_j\left[C_j\right] \tag{10}$$

Combining (9) and (10), we obtained

$$\sum_{i=1}^{M} k_j\left[C_j\right] = 14 \times 4.8 \times 10^{-11} \times \frac{[C_2Cl_4]}{[O_3]} \times [Cl] \tag{11}$$

In the manuscript, $\sum_{j=1}^{M} k_j\left[C_j\right]$ was defined as the depletion rate coefficient for O_3. Based on the linear relation between O_3 and C_2Cl_4 (Fig. 9b in the manuscript):

$$[O_3] = -40 + 14 \times [C_2Cl_4] \tag{12}$$

The ratio of C_2Cl_4/O_3 was of the magnitude of 10^{-1}. Using this ratio value for (11), we obtained the depletion rate coefficient of O_3 as follows:

$$\sum_{j=1}^{M} k_j\left[C_j\right] \sim 10^{-10} \times [Cl] \tag{13}$$

which is Eq. (1) in the manuscript.

If we utilize the Hg°-C_2H_2 correlation instead of the Hg°-C_2Cl_4 one, then the depletion rate of Hg° can be expressed as

$$\frac{d[Hg^\circ]}{dt} = \frac{d[Hg^\circ]}{d[C_2H_2]} \times \frac{d[C_2H_2]}{dt} \tag{14}$$

where $\frac{d[Hg^o]}{d[C_2H_2]}$ is approximated to be the discreet form $\frac{\Delta[Hg^o]}{\Delta[C_2H_2]}$, which is the slope value (0.38 ppqv/pptv) of the Hg°-C_2H_2 linear correlation (Fig. 12a in the manuscript), and $\frac{d[C_2H_2]}{dt}$ is expressed as:

$$\frac{d[C_2H_2]}{dt} = -\left(k_{C_2H_2-Cl}[Cl] + k_{C_2H_2-Brl}[Br] + k_{C_2H_2-OH}[OH]\right) \times [C_2H_2] \tag{15}$$

where $k_{C_2H_2-X}$ is the reaction rate constant for the reaction of C_2H_2 with X (X stands for Cl, Br, or OH). As stated in the manuscript, we used the k value for C_2H_2 reactions with Cl and OH from Sander et al. (2002) and that with Br from Atkinson et al. (2006). At a temperature of 254 K the values are 2.48×10^{-10} cm^3 molecule^{-1} s^{-1}, 5.95×10^{-13} cm^3 molecule^{-1} s^{-1}, and 3.59×10^{-14} cm^3 molecule^{-1} s^{-1}, respectively. Therefore Eq. (14) can be expressed as:

$$\frac{d[Hg^o]}{dt} = -0.38 \times \left(5.95 \times 10^{-13}[OH] + 2.48 \times 10^{-10}[Cl] + 3.59 \times 10^{-14}[Br]\right)[C_2H_2] \tag{16}$$

Combining (4) and (16) we obtained the Hg° depletion rate coefficient as follows:

$$\sum_{i=1}^{N} k_i[C_i] = 0.38 \times \left(5.95 \times 10^{-13}[OH] + 2.48 \times 10^{-10}[Cl] + 3.59 \times 10^{-14}[Br]\right) \times \frac{[C_2H_2]}{[Hg^o]} \tag{17}$$

Based on the linear relation between Hg° and C_2H_2 (Fig. 12a in the manuscript):

$$[Hg^\circ] = -4.8 + 0.38 \times [C_2H_2] \tag{18}$$

The ratio of C_2H_2/Hg° was on the order of 10^0. Using this ratio value for (17), we obtained the Hg° depletion rate coefficient:

$$\sum_{i=1}^{N} k_i[C_i] \sim 10^{-13}[OH] + 10^{-10}[Cl] + 10^{-14}[Br] \tag{19}$$

which is Eq. (5) in the manuscript.

Similarly, we used the O_3-C_2H_2 correlation instead of the O_3-C_2Cl_4 one, the depletion rate of O_3 can be expressed as:

$$\frac{d[O_3]}{dt} = \frac{d[O_3]}{d[C_2H_2]} \times \frac{d[C_2H_2]}{dt} \tag{20}$$

where $\frac{d[O_3]}{d[C_2H_2]}$ is approximated to be the discreet form $\frac{\Delta[O_3]}{\Delta[C_2H_2]}$, which is the slope value (0.1 ppbv/pptv) of the O_3-C_2H_2 linear correlation (Fig. 12b in the manuscript). Combining this slope value together with (15), Eq. (20) can be expressed as:

$$\frac{d[O_3]}{dt} = -0.1 \times (5.95 \times 10^{-13}[OH] + 2.48 \times 10^{-10}[Cl] + 3.59 \times 10^{-14}[Br])[C_2H_2] \tag{21}$$

Combining (10) and (21) we obtained the O_3 depletion rate coefficient as follows:

$$\sum_{j=1}^{M} k_j[C_j] = 0.1 \times (5.95 \times 10^{-13}[OH] + 2.48 \times 10^{-10}[Cl] + 3.59 \times 10^{-14}[Br]) \times \frac{[C_2H_2]}{[O_3]} \tag{22}$$

Based on the linear relation between O_3 and C_2H_2 (Fig. 12a in the manuscript):

$$[O_3] = -2.5 + 0.1 \times [C_2H_2] \tag{23}$$

The ratio of C_2H_2/O_3 was on the order of magnitude of 10. Using this ratio value for (22), we obtained the O_3 depletion rate coefficient as follows:

$$\sum_{j=1}^{M} k_j[C_j] \sim 10^{-13}[OH] + 10^{-10}[Cl] + 10^{-14}[Br] \tag{24}$$

which is Eq. (4) in the manuscript.

References

Ariya, P.A., Catoire, V., Sander, R., Niki, H., Harris, G.W.: Trichloroethene and tetrachloroethene: tropospheric probes for Cl- and Br-atom chemistry during the polar sunrise. Tellus Ser. B **49**, 583–591 (1997)

Ariya, P., Niki, H., Harris, G.W., Anlauf, K.G., Worthy, D.E.J.: Polar sunrise experiment 1995: hydrocarbon measurements and tropospheric Cl and Br atoms chemistry. Atmos. Environ. **33**, 931–938 (1999)

Ariya, P.A., Khalizov, A.F., Gidas, A.: Reaction of gaseous mercury with atomic and molecular malogens: kinetics, product studies, and atmospheric implications. J. Phys. Chem. A **106**(32), 7310–7320 (2002)

Ariya, P., Dastoor, A., Amyot, M., Schroeder, W., Barrie, L., Anlauf, K., Raofie, F., Ryzhkov, A., Davignon, D., Lalonde, J., Steffen, A.: The Arctic: a sink for mercury. Tellus Ser. B **56**(5), 397–403 (2004)

Atkinson, R., Baulch, D.L., Cox, R.A., Crowley, J.N., Hampson, R.F., Hynes, R.G., Jenkin, M.E., Rossi, M. J., Troe, J.: Evaluated kinetic and photochemical data for atmospheric chemistry: Volume II – gas phase reactions of organic species. Atmos. Chem. Phys. **6**, 3625–4055 (2006)

Banic, C.M., Beauchamp, S.T., Tordon, R.J., Schroeder, W.H., Steffen, A., Anlauf, K.A., Wong, H.K.T.: Vertical distribution of gaseous elemental mercury in Canada. J. Geophys. Res. **108**, 4264 (2003). doi:10.1029/2002JD002116

Berg, T., Sommar, J., Wangberg, I., Gardfeldt, K., Munthe, J., et al.: Arctic mercury depletion events at two elevations as observed at the Zeppelin Station and Dirigible Italia, Ny-Alesund, spring 2002. J. Phys.-Paris **107**, 151–154 (2003)

Bottenheim, J.W., Barrie, L.A., Atlas, E., Heidt, L.E., Niki, H., Rasmussen, R.A., Shepson, P.B.: Depletion of lower tropospheric ozone during Arctic spring: the polar sunrise experiment 1988. J. Geophys. Res. **95**(D11), 18,555–18,568 (1990)

Bottenheim, J.W., Fuentes, J.D., Tarasick, D.W., Anlauf, K.G.: Ozone in the Arctic lower troposphere during winter and spring 2000 (ALERT2000). Atmos. Environ. **36**, 2535–2544 (2002)

Boudries, H., Bottenheim, J.W., Cuimbaud, C., Grannas, A.M., Shepson, P.B., Houdier, S., Perrier, S.: and Dominé: distriubtion and trends of oxugenated hydrocarbons in the high Arctic derived frommeasurements in the atmospheric boundary layer and interstitial snow air during the ALERT2000 field campaign. Atmos. Environ. **36**, 2573–2583 (2002)

Brooks, S.B., Saiz-Lopez, A., Skov, H., Lindberg, S.E., Plane, J.M.C., Goodsite, M.E.G.: The mass balance of mercury in the springtime arctic environment. Geophys. Res. Lett. **33**, L13812 (2006). doi:10.1029/2005GL025525,2006

Calvert, J.G., Lindberg, S.E.: A modeling study of the mechanism of the halogen-ozone-mercury homogeneous reactions in the troposphere during the polar spring. Atmos. Environ. **37**, 4467–4481 (2003)

Cavender, A.E., Biesenthal, T.A., Bottenheim, J.W., Shepson, P.B.: Volatile organic compound ratios as probes of halogen atom chemistry in the Arctic. Atmos. Chem. Phys. **8**, 1737–1750 (2008)

Colman, J.J., Swanson, A.L., Meinardi, S., Sive, B.C., Blake, D.R., Rowland, F.S.: Description of the analysis of a wide range of volatile organic compounds in whole air samples collected during PEM-Tropics A and B. Anal. Chem. **73**, 3723–3731 (2001)

Ebinghaus, R., Slemr, F.: Aircraft measurements of atmospheric mercury over southern and eastern Germany. Atmos. Environ. **34**, 895–903 (2000)

Ebinghaus, R., Kock, H.H., Temme, C., et al.: Antarctic springtime depletion of atmospheric mercury. Environ. Sci. Technol. **36**(6), 1238–1244 (2002)

Eneroth, K., Holmén, K., Berg, T., Schmidbauer, N., Solberg, S.: Springtime depletion of tropospheric ozone, gaseous elemental mercury and non-methane hydrocarbons in the European Arctic, and its relation to atmospheric transport. Atmos. Environ. **41**, 8511–8526 (2007)

Friedli, H.R., Radke, L.F., Prescott, R., Li, P., Woo, J.-H., Carmichael, G.R.: Mercury in the atmosphere around Japan, Korea, and China as observed during the 2001 ACE-Asia field campaign: measurements, distributions, sources, and implications. J. Geophys. Res. **109**, D19S25 (2004). doi:10.1029/2003JD004244

Fuelberg, H.E., Loring Jr., R.O., Watson, M.V., Sinha, M.C., Pickering, K.E., Thompson, A.M., Sachse, G. W., Blake, D.R., Schoeberl, M.R.: TRACE-A trajectory Intercomparison 2. Isentropic and kinematic methods. J. Geophys. Res. **101**, 23927–23939 (1996)

Fuelberg, H.E., Hannan, J.R., van Velthoven, P.F.J., Browell, E.V., Bieberbach Jr., G., Knabb, R.D., Gregory, G.L., Pickering, K.E., Selkirk, H.B.: A meteorological overview of the SONEX period. J. Geophys. Res. **105**, 3633–3651 (2000)

Goodsite, M.E., Plane, J.M.C., Skov, H.: A theoretical study of the oxidation of Hg-0 to $HgBr_2$ in the troposphere. Environ. Sci. Technol. **38**, 1772–1776 (2004)

Jobson, B.T., Niki, H., Yokouchi, Y., Bottenheim, J., Hopper, F., Leaitch, R.: Measurements of C2-C6 hydrocarbons during the polar sunrise 1992 experiment: evidence for Cl atom and Br atom chemistry. J. Geophys. Res. **99**(D12), 25,355–25,368 (1994)

Kim, S.Y., Talbot, R., Mao, H., Blake, D., Weinheimer, A., Huey, G.: Chemical transformations of Hg° during Arctic mercury depletion events sampled from the NASA DC-8. Atmos. Chem. Phys. Discuss. **10**, 10077–10112 (2010)

Lindberg, S.E., Brooks, S.B., Lin, C.J., Scott, K., Meyers, T., Chambers, L., Landis, M., Stevens, R.K.: Formation of reactive gaseous mercury in the Arctic: evidence of oxidation of Hg^0 to gas-phase Hg-II compounds after Arctic sunrise. Water Air Soil Pollut. **1**, 295–302 (2001)

Lu, J.Y., Schroeder, W.H., Barrie, L.A., Steffen, A., Welch, H.E., Martin, K., Lockhart, L., Hunt, R.V., Boila, G., Richter, A.: Magnification of atmospheric mercury deposition to polar regions in springtime: the link to tropospheric ozone depletion chemistry. Geophys. Res. Lett. **28**, 3219–3222 (2001)

Mao, H., Talbot, R.: O_3 and CO in New England: temporal variations and relationships. J. Geophys. Res. **109**, D21304 (2004). doi:10.1029/2004JD004913

Martin, B.D., Fuelberg, H.E., Blake, N.J., Crawford, J.H., Logan, J.A., Blake, D.R., Sachse, G.W.: Long range transport of Asian outflow to the equatorial Pacific. J. Geophys. Res. **108**(D2), 8322 (2002). doi:10.1029/2001JD001418

Potosnak, M.J., Wofsy, S.C., Denning, A.S., Conway, T.J., Munger, J.W., Barnes, D.H.: Influence of biotic exchange and combustion sources on atmospheric CO_2 concentrations in New England from observations at a forest flux tower. J. Geophys. Res. **104**, 9561–9569 (1999)

Radke, L.F., Friedli, H.R., Heikes, B.G.: Atmospheric mercury over the NE Pacific during ITCT2K2: gradients, residence time, stratosphere-troposphere exchange, and long-range transport. J. Geophys. Res. **112**, D19305 (2007). doi:10.1029/2005JD005828

Ridley, B.A., Grahek, F.E., Walega, J.G.: A small, high-sensitivity, medium-response ozone detector suitable for measurements from light aircraft. J. Atmos. Oceanic Technol. **9**, 142–148 (1992)

Ridley, B.A., Atlas, E.L., Montzka, D.D., et al.: Ozone depletion events in the high latitude surface layer during the TOPSE aircraft program. J. Geophys. Res. **108**(D4), 8356 (2003). doi:10.1029/2001JD001507

Sander, S.P., Finlayson-Pitts, B.J., Friedli, R.R., et al.: Chemical Kinetics and Photochemical Data for Use in Atmospheric Studies, Evaluation Number 14, JPL Publication 02–25. Jet Propulsion Laboratory, Pasadena, CA (2002)

Schroeder, W.H., Anlauf, K.G., Barrie, L.A., Lu, J.Y., Steffen, A., Schneeberger, D.R., Berg, T.: Arctic springtime depletion of mercury. Nature **394**, 331–332 (1998)

Sive, B. C., Blake, N. J., Wingenter, O. W., Blake, D. R., and Rowland, F. S.: nonmethane hydrocarbon, halocarbon, and alkyl nitrate measurements during TOPSE: Evidence of halogen atom chemistry. 23rd Annual Midwest Environmental Chemistry Workshop, Western Michigan University, October 7–8 (2000)

Skov, H., Christensen, J., Goodsite, M., Heidam, N.Z., Jensen, B., Wahlin, P., Geernaert, G.: Fate of elemental mercury in the Arctic during atmospheric mercury depletion episodes and the load of atmospheric mercury to the Arctic. Environ. Sci. Technol. **38**, 2373–2382 (2004)

Sprovieri, F., Pirrone, N., Landis, M.S., Stevens, R.K.: Atmospheric mercury behavior at different altitudes at Ny Alesund during Spring 2003. Atmos. Environ. **39**, 7646–7656 (2005)

Swartzendruber, P.C., Chand, D., Jaffe, D.A., Smith, J., et al.: Vertical distribution of mercury, CO, ozone and aerosol scattering coefficient in the Pacific Northwest during the spring 2006 INTEX-B campaign. J. Geophys. Res. **113**, D10305 (2008). doi:10.1029/2007JD009579

Tackett, P.J., Cavender, A.E., Keil, A.D., Shepson, P.B., Bottenheim, J.W., Morin, S., Deary, J., Steffen, A., Doerge, C.: A study of the vertical scale of halogen chemistry in the Arctic troposphere during polar sunrise at Barrow Alaska. J. Geophys. Res. **112**, D07306 (2007). doi:10.1029/2006JD007785

Talbot, R., Mao, H., Scheuer, E., Dibb, J., Avery, M.: Total depletion of Hg° in the upper troposphere - lower stratosphere. Geophys. Res. Lett. **34**, L23804 (2007). doi:10.1029/2007GL031366

Talbot, R., Mao, H., Scheuer, E., Dibb, J., Avery, M., Browell, E., Sachse, G., Vay, S., Blake, D., Huey, G., Fuelberg, H.: Factors influencing the large-scale distribution of Hg° in the Mexico City area and over the North Pacific. Atmos. Chem. Phys. **8**, 2103–2114 (2008)

Thuner, L.P., Barnes, I., Becker, K.H., Wallington, T.J., Christensen, L.K., Orlando, J.J., Ramacher, B.: Atmospheric chemistry of tetrachloroethene ($Cl_2C = CCl_2$): products of chlorine atom initiated oxidation. J. Phys. Chem. A **103**, 8657–8663 (1999)

Von Glasow, R.: Sun, sea and ozone destruction. Nature **453**, 1195–1196 (2008)